Toll-like Receptor 4 Deficiency Promotes the Alternative Activation of Adipose Tissue Macrophages

Jeb S. Orr, Michael J. Puglisi, Kate L.J. Ellacott, Carey N. Lumeng, David H. Wasserman, and Alyssa H. Hasty

Obesity is characterized by adipose tissue (AT) macrophage (ATM) accumulation, which promotes AT inflammation and dysfunction. Toll-like receptor 4 (TLR4) deficiency attenuates AT inflammation in obesity but does not impede the accumulation of ATMs. The purpose of the current study was to determine whether TLR4 deficiency alters ATM polarization. TLR4$^{-/-}$ and wild-type mice were fed a low-fat, high-monounsaturated fat (HF^{MUFA}), or a high-saturated fat (HF^{SFA}) diet for 16 weeks. Further, we used a bone marrow transplant model to determine the influence of hematopoietic cell TLR4 signaling. The metabolic and inflammatory responses to high-fat feeding and ATM phenotype were assessed. Global and hematopoietic cell TLR4 deficiency, irrespective of recipient genotype, produced a shift in ATM phenotype toward an alternatively activated state, which was accompanied by reduced AT inflammation. Despite the observed shift in ATM phenotype, neither global nor hematopoietic cell TLR4 deficiency influenced systemic insulin sensitivity after high-fat feeding. Results of the current study suggest that TLR4 directly influences ATM polarization but question the relevance of TLR4 signaling to systemic glucose homeostasis in obesity. *Diabetes* **61:2718–2727, 2012**

I n 1993, Hotamisligil et al. (1) first demonstrated that tumor necrosis factor-α (TNF-α) is expressed in adipose tissue (AT) and elevated in various rodent models of obesity. Subsequent research has led to the characterization of the obese state as one of chronic low-grade inflammation, which contributes to the development of systemic insulin resistance (IR) (2). Implicit in the idea that inflammatory status links obesity and IR is the notion that signaling pathways exist whereby the recognition of nutrient excess elicits an immune response. Confirmation of such a mechanism came with the discovery of the first human homolog of the *Drosophila* Toll receptor, Toll-like receptor 4 (TLR4) (3), and the subsequent finding that saturated fatty acids (SFAs) were capable of activating nuclear factor-κB in a TLR4-dependent manner (4).

Numerous studies have explored the role of TLR4 signaling in the metabolic consequences of diet-induced obesity (DIO). Despite contradictory findings with respect to the influence of TLR4 on weight gain, the present literature consistently demonstrates that TLR4 deficiency reduces AT inflammation and hepatic steatosis after a high-fat (HF)

diet (HFD) (5–7). Thus, the available evidence suggests that the beneficial metabolic effects of TLR4 deficiency may be due, in part, to the preservation of AT function during the development of DIO.

The capacity of AT to act as an effective buffer against lipid "spillover" into metabolic tissues (e.g., skeletal muscle, liver, kidneys) relies on its ability to expand, via hypertrophy and hyperplasia, in response to chronic overnutrition. This process involves the coordinated interaction of various cell populations comprising the AT stromal vascular fraction (SVF), including AT macrophages (ATMs), which have received a great deal of attention due to their progressive accumulation during AT expansion as well as their high inflammatory potential and influence on AT insulin sensitivity and angiogenesis (8,9). It is interesting to note that although hematopoietic or global TLR4 deficiency results in decreased AT inflammation, the prevalence of ATMs is not reliably reduced (10–13), thus raising questions about the influence of TLR4 signaling on ATM phenotype.

Recently, the phenotypic diversity of ATMs has come to the forefront. In keeping with the T helper 1 and 2 (Th1/Th2) paradigm, the current literature relies on the M1/M2 nomenclature to refer to classically and alternatively activated macrophages, respectively. The prevailing model of ATM polarization holds that "resident" ATMs display an alternatively activated phenotype, whereas macrophages recruited to AT during the onset of obesity exhibit a predominantly M1 "classical activation" state (14). This obesity-associated shift in ATM polarization leads to a pronounced increase in the ratio of M1-to-M2 ATMs, thus promoting an inflammatory state within the AT.

Although the direct influence of TLR4 signaling on ATM polarization remains unclear, several lines of evidence point to a potential role: *1*) TLR4 deficiency attenuates obesity-associated AT inflammation and IR in the face of ATM accumulation (10–13); *2*) recruited M1 ATMs express high levels of TLR4, whereas M2 ATMs highly express suppression of tumorigenicity 2 (ST2), a negative regulator of TLR4 signaling (15); *3*) overexpression of activating transcription factor-3 (ATF3), a transcriptional repressor of TLR4 signaling, reduces M1 polarization of ATMs after 4 weeks of HF feeding (12). Taken together, the above evidence suggests that TLR4 deficiency may attenuate the inflammatory response to HF feeding, in part, by promoting the alternative activation of ATMs. Accordingly, the purpose of the current study was to test the hypothesis that TLR4 deficiency would promote the alternative activation of ATMs, which would be associated with a reduction in AT inflammation and systemic IR.

RESEARCH DESIGN AND METHODS

Diets. The current study used the following dietary treatments: low fat (LF; 10.5% kcal from fat), high-monounsaturated fat (HF^{MUFA}; 45% kcal from fat, of

which 68.5% were MUFA), and high-saturated fat (HF^{SFA}; 45% kcal from fat, of which 91.5% were SFAs). Corn starch served as the predominant carbohydrate source to minimize the potential confounding influence of the increased sucrose content of commercial HFDs. All diets were purchased from Research Diets (New Brunswick, NJ). Mice had free access to water, and average daily food intake was assessed weekly in each cage of mice.

Mice. All animal care and experimental procedures were approved by the Vanderbilt University Institutional Animal Care and Usage Committee. Only male mice were included in the current study. TLR4$^{-/-}$ mice on a C57BL/6 background were provided by Satoshi Uematsu and Shizuo Akira (Department of Host Defense, University of Osaka, Japan) and subsequently bred with C57BL/6 mice from our colony. TLR4$^{+/-}$ mice were crossed, and the TLR4$^{-/-}$ offspring were interbred to obtain the TLR4$^{-/-}$ mice included in the current study (n = 13 LF, 13 HF^{MUFA}, and 13 HF^{SFA}). C57BL/6, wild-type (WT) control mice (n = 15 LF, 14 HF^{MUFA}, and 16 HF^{SFA}) were from our colony or purchased from Jackson Laboratory (Bar Harbor, ME). WT mice obtained from Jackson Laboratory were given a 1-week acclimation period before being included in the study. Similar results were obtained regardless of the source of WT mice.

Bone marrow transplant. After lethal irradiation, male WT and TLR4$^{-/-}$ mice were reconstituted with bone marrow (BM) from age-matched male WT or TLR4$^{-/-}$ donor mice, as previously described (13). WT recipients reconstituted with WT and TLR4$^{-/-}$ BM are denoted as WT^{WTBM} and WT$^{TLR4-/-BM}$, respectively. TLR4$^{-/-}$ recipients reconstituted with WT and TLR4$^{-/-}$ BM are denoted as TLR4$^{-/-WTBM}$ and TLR4$^{-/-TLR4-/-BM}$, respectively.

Body composition. Total body fat, muscle, and free fluid were measured via nuclear magnetic resonance using a Bruker Minispec (Woodlands, TX) in the Vanderbilt University Mouse Metabolic Phenotyping Center (MMPC).

Blood collection and plasma analyses. Fasting blood glucose, plasma insulin, adiponectin, total cholesterol, free fatty acids (FFA), and triglyceride (TG) concentrations were measured, as previously described (16). Plasma leptin was assessed via radioimmunoassay in the Vanderbilt Hormone Assay and Analytical Services Core.

Adipocyte and SVF isolation. Mice were killed, and blood was removed via central perfusion. Perigonadal AT depots were minced in Dulbecco's PBS supplemented with 0.5% BSA. Subsequently, CaCl$_2$ and type II collagenase were added to a final concentration of 5 mmol/L and 1 mg/mL, respectively. Tissue homogenates were incubated at 37°C for 20 min with shaking. After filtration and centrifugation, buoyant adipocytes were removed, washed twice, and collected as the adipocyte fraction. The remaining cell pellet was resuspended in ACK lysis buffer, washed, and collected as the SVF.

Fluorescence-activated cell sorter analysis. SVF cells were incubated with Fc block (BD Biosciences) on ice for 15 min. Subsequently, primary fluorophore-conjugated antibodies against F4/80 (eBioscience) and Mgl1 (AbD Serotec) were added, and the cell suspensions were incubated at 4°C for 30 min. Samples were processed in the Vanderbilt Flow Cytometry Core using an LSRII flow cytometer (BD Biosciences) and analyzed using FlowJo software (Tree Star, Inc.).

Peritoneal macrophage polarization. Peritoneal macrophages (PMs) were harvested from age-matched, male WT and TLR4$^{-/-}$ mice, as previously described (17). Subsequently, PMs were treated with a combination of interferon-γ (100 units/mL) and TNF-α (500 units/mL) or interleukin (IL)-13 (40 ng/mL) for 24 h to elicit M1 or M2 polarization, respectively.

mRNA expression. RNA isolation and cDNA synthesis were performed as previously described (18). Real-time RT-PCR was performed on an iQ5 cycler (Bio-Rad, Hercules, CA). Primer-probe sets were purchased from Applied Biosystem's Assays-on-Demand (catalog numbers available upon request). Expression was normalized relative to 18S or glyceraldehyde-3-phosphate dehydrogenase using the ΔΔC$_t$ method.

Liver TG concentrations. Liver tissue TG concentrations were determined via gas chromatography, as previously described (19).

Oil Red O staining. Neutral lipid accumulation in liver sections was visualized by Oil Red O (ORO) staining, as previously described (20).

Glucose and insulin tolerance tests. After a 5-h fast, blood was collected from the tail vein, and blood glucose was measured using a Lifescan OneTouch Ultra glucometer (Johnson & Johnson, Northridge, CA). Subsequently, blood glucose was measured 15, 30, 45, 60, 90, and 120 min after an intraperitoneal injection of glucose (1 g/kg) or insulin (0.375 IU/kg) to assess glucose and insulin tolerance, respectively.

Hyperinsulinemic-euglycemic clamp. Hyperinsulinemic-euglycemic clamps were performed in 5-h fasted mice at the Vanderbilt MMPC, as previously described (21). In preparation for clamps, catheters were implanted in the carotid artery for blood sampling and in the right jugular vein for blood intravenous infusion at least 5 days before the study. After collection of fasting arterial blood, insulin was infused (4 mU/kg/min) for 120 min. Blood glucose was clamped at 120–130 mg/dL by a variable glucose infusion. Steady-state glucose fluxes were measured using [3-^{3}H]glucose (22). Tissue-specific glucose metabolic index was measured using 2[^{14}C]deoxyglucose ([^{14}C]2DG), as described previously (23).

Statistics. Statistical analyses were performed using GraphPad Prism 4.03 (GraphPad, La Jolla, CA) and JMP 8.0.2 (SAS Institute, Inc., Cary, NC) software. Non-normally distributed data were log-transformed. Changes in dependent variables over time were assessed using repeated-measures ANOVA with the Bonferroni post hoc test. Diet and genotype effects, as well as diet × genotype interactions were determined by two-way ANOVA with the Tukey honestly significant difference post hoc test. Comparisons within BM transplant (BMT) recipient groups were performed using unpaired t tests. The Grubbs test was used to detect significant outliers, which were removed before statistical analysis. Data are expressed as mean ± SEM, and significance was set at $P < 0.05$.

RESULTS

Body weight and body fat gain was slightly reduced by TLR4 deficiency. In light of previous studies, suggesting that SFAs act as a ligand for TLR4 (4,24,25), we chose an experimental design whereby the diet-treatment groups differed in fat content (i.e., 10 vs. 45% kcal from fat), as well as fatty acid profile (i.e., HF^{MUFA} vs. HF^{SFA}). Although HF^{MUFA} and HF^{SFA} feeding induced dramatic weight gain in WT and TLR4$^{-/-}$ mice, TLR4 deficiency blunted weight gain in response to both HFDs (Fig. 1A). Consistent with the observed differences in weight gain, food intake was significantly reduced in TLR4$^{-/-}$ compared with WT counterparts (Supplementary Fig. 1A). Because TLR4 signaling has previously been implicated in the development of hypothalamic inflammation in response to HF feeding (26), we assessed hypothalamic inflammatory gene expression to determine whether alterations in hypothalamic inflammation are associated with the observed reduction in food intake by TLR4-deficient mice. TLR4$^{-/-}$ mice exhibited significantly greater hypothalamic Il10 expression after HF^{SFA} feeding; however, hypothalamic expression of Tnfa, Il6, chemokine (C-C motif) ligand (CCL) 2 (Ccl2), and Il1b was unchanged after HF feeding and was not influenced by genotype (Supplementary Fig. 1B–F). Despite producing similar weight gain, significant diet effects were observed with respect to total adiposity, as HF^{SFA} feeding induced the greatest increases in body fat (Supplementary Table 1). In contrast to total body fat, TLR4 deficiency reduced visceral fat accumulation, as significant genotype effects were present for perigonadal and perirenal fat pad weight (Supplementary Table 1). As expected, HF feeding produced significant elevations in plasma leptin concentrations; however, TLR4 deficiency attenuated this increase in HF^{SFA}-fed mice (Supplementary Table 2). There was a significant diet × genotype interaction for plasma adiponectin, as concentrations were reduced in TLR4$^{-/-}$ compared with WT mice fed the LF diet. In addition, the HF^{SFA} diet reduced adiponectin concentrations regardless of genotype (Supplementary Table 2).

Diet effects were observed with respect to fasting plasma lipid and lipoprotein concentrations, whereas genotype did not influence this response (Supplementary Table 2). Total cholesterol concentrations were significantly reduced in LF-fed mice, whereas HF^{MUFA}-fed mice presented the lowest concentrations of FFA and TG. Overall, these data indicate a slight attenuation in weight gain and adiposity for TLR4$^{-/-}$ mice in response to an HFD irrespective of dietary fatty acid composition.

TLR4 deficiency reduced liver TG after HF^{SFA} feeding. HF feeding induced hepatic steatosis, which was significantly attenuated in TLR4-deficient mice (Fig. 1B). ORO staining of liver sections allowed for a visual display of this
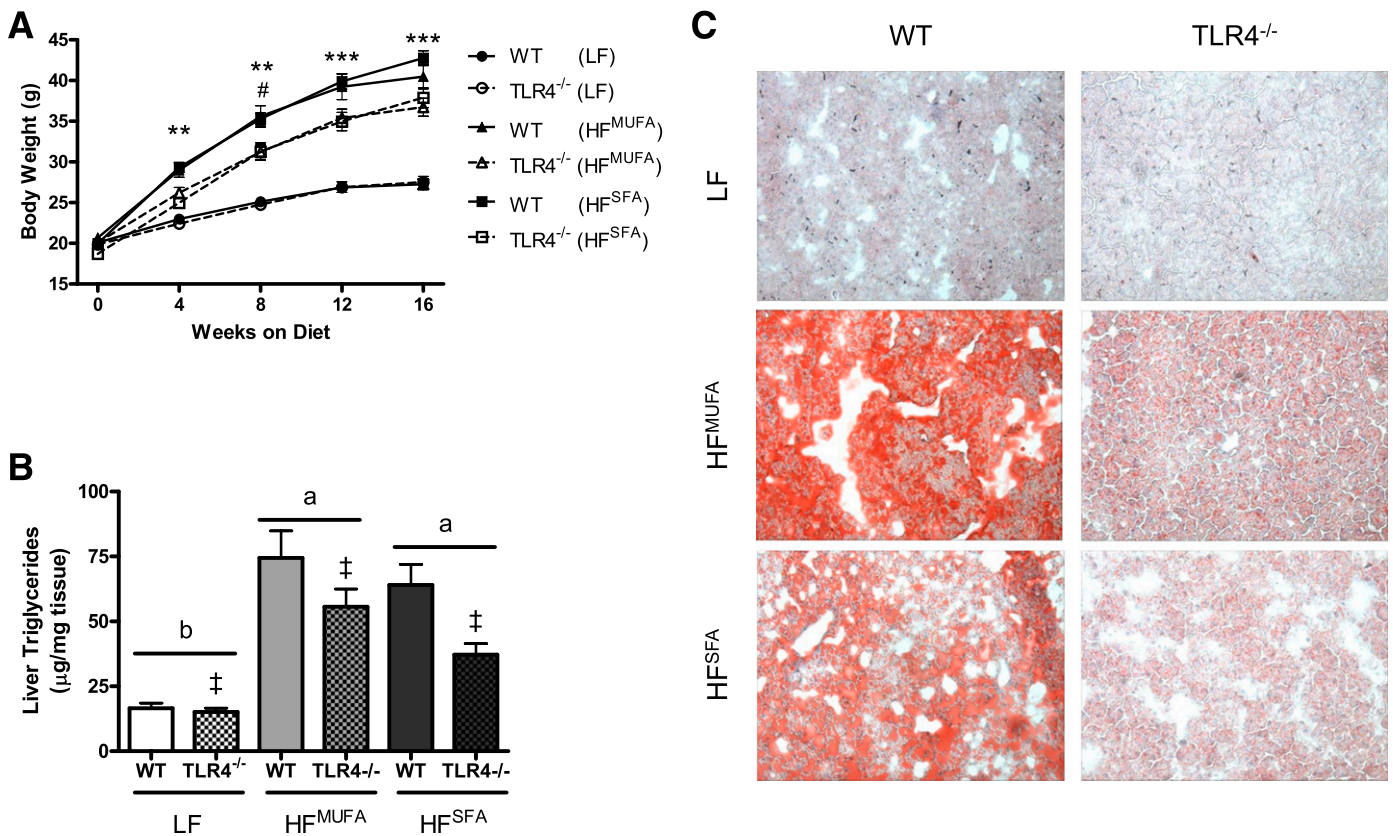
FIG. 1. TLR4 deficiency attenuates weight gain and hepatic TG accumulation after HF feeding. *A*: WT and TLR4-deficient mice display similar growth curves on a LF diet, whereas weight gain is attenuated in TLR4$^{-/-}$ mice after HF^{MUFA} and HF^{SFA} feeding (n = 13–15 for all diet conditions). *B*: TLR4 deficiency reduces HF-feeding–induced hepatic TG accumulation (n = 13–16). *C*: Representative images of ORO-stained liver sections. Data are presented as mean ± SEM. **P < 0.01 and ***P < 0.001 for WT HF^{SFA} vs. TLR4$^{-/-}$ HF^{SFA}; #*P* < 0.05 for WT HF^{MUFA} vs. TLR4$^{-/-}$ HF^{MUFA}; ‡*P* < 0.01 for genotype effect; and *P* < 0.05 for groups not connected by the same letter. (A high-quality digital representation of this figure is available in the online issue.)

pattern (Fig. 1*C*). Lipid metabolism in the liver was assessed by analyzing hepatic mRNA expression of stearoyl-coenzyme A desaturase 1 (*Scd1*), sterol regulatory element binding transcription factor 1 (*Srebf1*), acyl-coenzyme A oxidase, palmitoyl (*Acox1*), and carnitine palmitoyltransferase 1a (*Cpt1a*) by real-time RT-PCR (Supplementary Fig. 2*A*–*D*). Although no main effects were present, a significant diet × genotype interaction was observed for *Scd1* as shown by significantly greater expression in LF TLR4$^{-/-}$ compared with WT counterparts. Expression of all other genes related to lipid metabolism was not affected by genotype or diet. Inflammatory status of the liver was determined by measuring hepatic gene expression of various inflammatory cytokines and chemokines (Supplementary Fig 2*E*–*H*). An interaction between diet and genotype was present for the inflammatory cytokine *Tnfa* as shown by significantly reduced expression in TLR4$^{-/-}$ compared with WT counterparts fed the HF^{MUFA} diet. TLR4 deficiency attenuated CCL-3 (*Ccl3*) expression, which was significantly elevated after the HF^{MUFA} diet. Similarly, there was a trend for reduced *Ccl2* expression in TLR4$^{-/-}$ mice (*P* = 0.07 for genotype effect), which was increased after HF^{MUFA} feeding. *Il6* expression was not influenced by diet or genotype.

TLR4 deficiency attenuates AT inflammation. With regards to AT inflammation (Fig. 2), we observed trends for an effect of diet (*P* = 0.10) and genotype (*P* = 0.07) on *Tnfa* expression. Both HFDs led to elevated *Tnfa* expression, which was attenuated in TLR4-deficient mice. Relative

to the LF diet, HF^{SFA} feeding increased *Ccl3* and *Tlr2* expression regardless of genotype. Interestingly, expression of the chemokine *Ccl2* was significantly greater in HF^{SFA}-fed TLR4$^{-/-}$ mice than in WT mice. *Il6* and *Il10* expression was not influenced by diet or genotype.

TLR4 deficiency promotes M2 polarization of ATMs and PMs. ATM accumulation, as quantified by the macrophage markers F4/80 (*Emr1*; Fig. 3*A*) and cluster of differentiation (CD) 68 (*Cd68*; Fig. 3*B*), was significantly increased by both HFDs in WT and TLR4$^{-/-}$ mice. Likewise, WT and TLR4$^{-/-}$ mice displayed similar increases in the prevalence of Mac-2–positive crown-like structures in the AT after HF feeding (data not shown). To assess ATM polarization, several markers of classical (M1) and alternative (M2) activation were quantified by real-time RT-PCR (Fig. 3*C*–*H*). Significant genotype effects were observed for mannose receptor C type 1 (*Mrc1*), C-type lectin domain family 10 member A (*Clec10a*), and macrophage galactose *N*-acetyl-galactosamine specific lectin 2 (*Mgl2*) as shown by these M2 markers being upregulated in the absence of TLR4 expression. In the case of *Clec10a*, there was a significant diet × genotype interaction, such that expression was significantly greater in HF^{SFA}-fed TLR4$^{-/-}$ mice than in WT mice. CD 163 antigen (*Cd163*), inducible nitric oxide synthase 2 (*Nos2*), and arginase-1 (*Arg1*) expression were not influenced by diet or genotype (Fig. 3*F*–*H*). Fluorescence-activated cell sorter (FACS) analysis of the AT SVF revealed similar findings to the gene
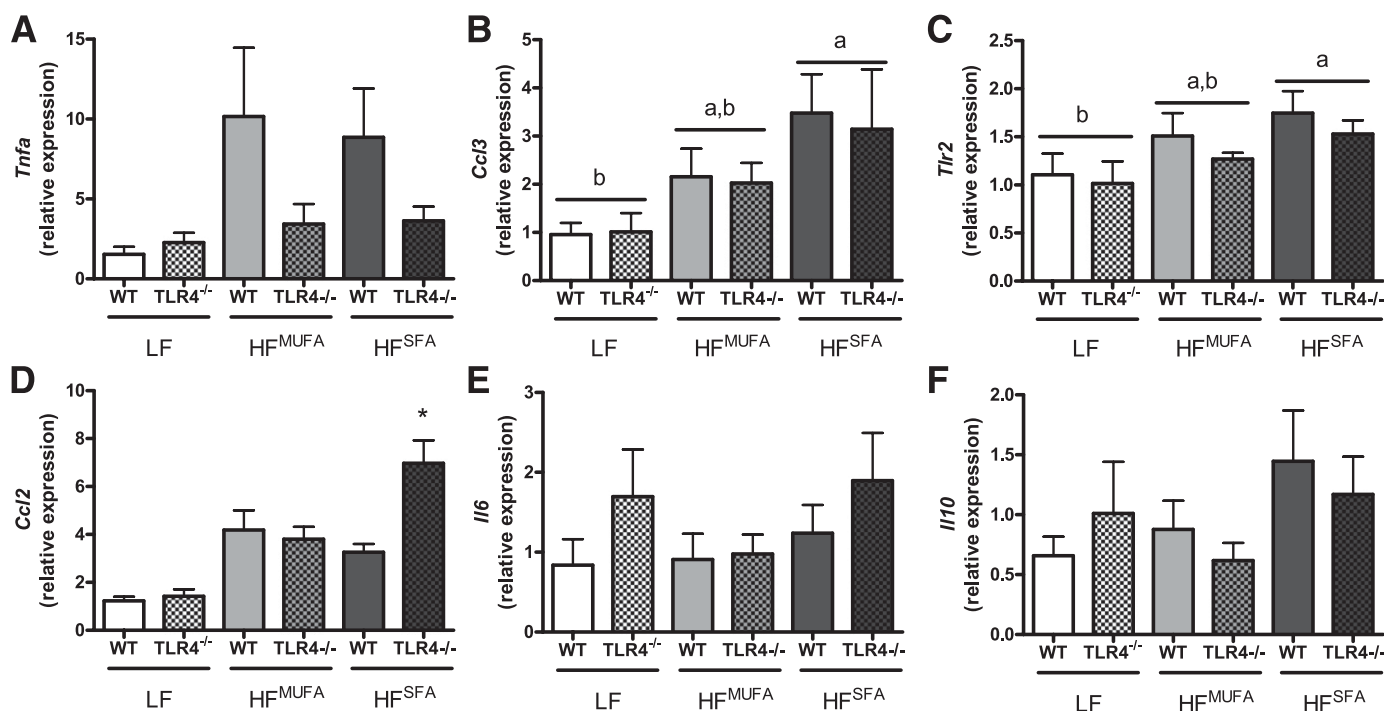
FIG. 2. AT inflammation. Real time RT-PCR was used to assess AT mRNA expression of *Tnfa* ($P = 0.07$ for genotype effect; $P < 0.10$ for diet effect) (*A*), *Ccl3* (*B*), *Tlr2* (*C*), *Ccl2* (*D*), *Il6* (*E*), and *Il10* (*F*). Data are presented as mean ± SEM ($n = 5$–16). *$P < 0.05$ for HF^{SFA} compared with LF in (*B*) and (*C*), *$P < 0.05$ for HF^{SFA} TLR4$^{-/-}$ compared with HF^{SFA} WT in (*D*), and $P < 0.05$ for groups not connected by the same letter.

expression data (Fig. 3*I–K*). HF^{SFA}-fed WT and TLR4$^{-/-}$ mice displayed similar numbers of ATMs as a percentage of SVF cells. However, consistent with the previously described elevation in *Clec10a* gene expression, the proportion of F4/80$^+$Mgl1$^+$ ATMs was significantly increased in TLR4-deficient mice. Finally, TLR4-deficient PMs appear skewed toward an alternatively activated gene expression profile as TLR4$^{-/-}$ PMs exhibited significantly greater *Il10* and *Arg1* expression compared with WT (Supplementary Fig. 3*B* and *C*) as well as significantly greater *Clec10a* expression and reduced *Nos2* expression after Th2 stimulation (Supplementary Fig. 3*A* and *F*).

Systemic insulin sensitivity is unaffected by TLR4 deficiency. Fasting plasma insulin and blood glucose concentrations were increased after HF feeding and were not influenced by genotype (Supplementary Table 2). Systemic insulin sensitivity was not influenced by genotype, because the glucose infusion rate required to maintain blood glucose between 120 and 130 mg/dL (Fig. 4*A*) during a hyperinsulinemic euglycemic clamp did not differ between HF^{SFA}-fed WT (29.9 ± 2.6 mg/kg/min) and TLR4$^{-/-}$ (26.5 ± 3.4 mg/kg/min) mice (Fig. 4*B*). Likewise, WT and TLR4$^{-/-}$ mice did not differ with respect to the rate of endogenous glucose appearance or glucose disappearance, suggesting comparable hepatic and peripheral insulin sensitivity, respectively (Fig. 4*C* and *D*). However, we observed significant reductions in insulin-stimulated glucose uptake at the gastrocnemius, superficial vastus lateralis, and AT of TLR4$^{-/-}$ mice compared with WT mice (Fig. 4*E*).

Hematopoietic cell TLR4 deficiency does not influence body weight, adiposity, or steatosis. In light of our data suggesting that, after HF^{SFA} feeding, TLR4 deficiency attenuates hepatic steatosis and AT inflammation concomitant to a shift in ATM polarization toward an M2 phenotype, we next sought to determine whether hematopoietic cell

TLR4 deficiency recapitulates the global TLR4$^{-/-}$ phenotype in response to HF^{SFA} feeding. Toward this aim, we conducted both the forward and reverse BMT, whereby lethally irradiated groups of WT and TLR4$^{-/-}$ recipients were reconstituted with WT or TLR4$^{-/-}$ BM (i.e., WT^{WTBM}, WT$^{TLR4-/-BM}$, TLR4$^{-/-WTBM}$, and TLR4$^{-/-TLR4-/-BM}$). Subsequently, mice were fed the HF^{SFA} diet for 20 weeks. Throughout the study, TLR4$^{-/-}$ recipient groups weighed less than their WT counterparts, irrespective of hematopoietic cell TLR4 expression (Supplementary Fig. 4*A*). Likewise, food consumption was significantly reduced in TLR4$^{-/-}$ compared with WT recipient groups and was not influenced by hematopoietic cell TLR4 expression (Supplementary Fig. 4*B*). Body fat and lean body mass were significantly reduced in TLR4$^{-/-}$ recipients, which accounted for the discrepant body weights between WT and TLR4$^{-/-}$ recipient groups (Supplementary Fig. 4*C* and *D*). Adiposity was similar between recipient groups and unaffected by hematopoietic cell TLR4 expression (Supplementary Fig. 4*E*).

Reflecting the differences in body weight between recipient groups, liver weight was significantly greater in WT recipient groups (Supplementary Fig. 5*A*). Given our observation of attenuated hepatic steatosis in TLR4$^{-/-}$ mice, we were surprised that TLR4 deficiency had no influence on hepatic TG accumulation in our BMT model (Supplementary Fig. 5*B* and *C*). Neither liver weight nor hepatic TG concentrations were influenced by hematopoietic cell TLR4 expression.

Hematopoietic cell TLR4 deficiency attenuates AT inflammation in WT recipients. To ascertain the influence of hematopoietic and parenchymal TLR4 deficiency on AT inflammation, the expression of various chemokines and cytokines were determined separately in isolated SVF and adipocyte fractions from the perigonadal AT. In the adipocyte fraction of WT$^{TLR-/-BM}$, *Tnfa* and *Ccl3* gene
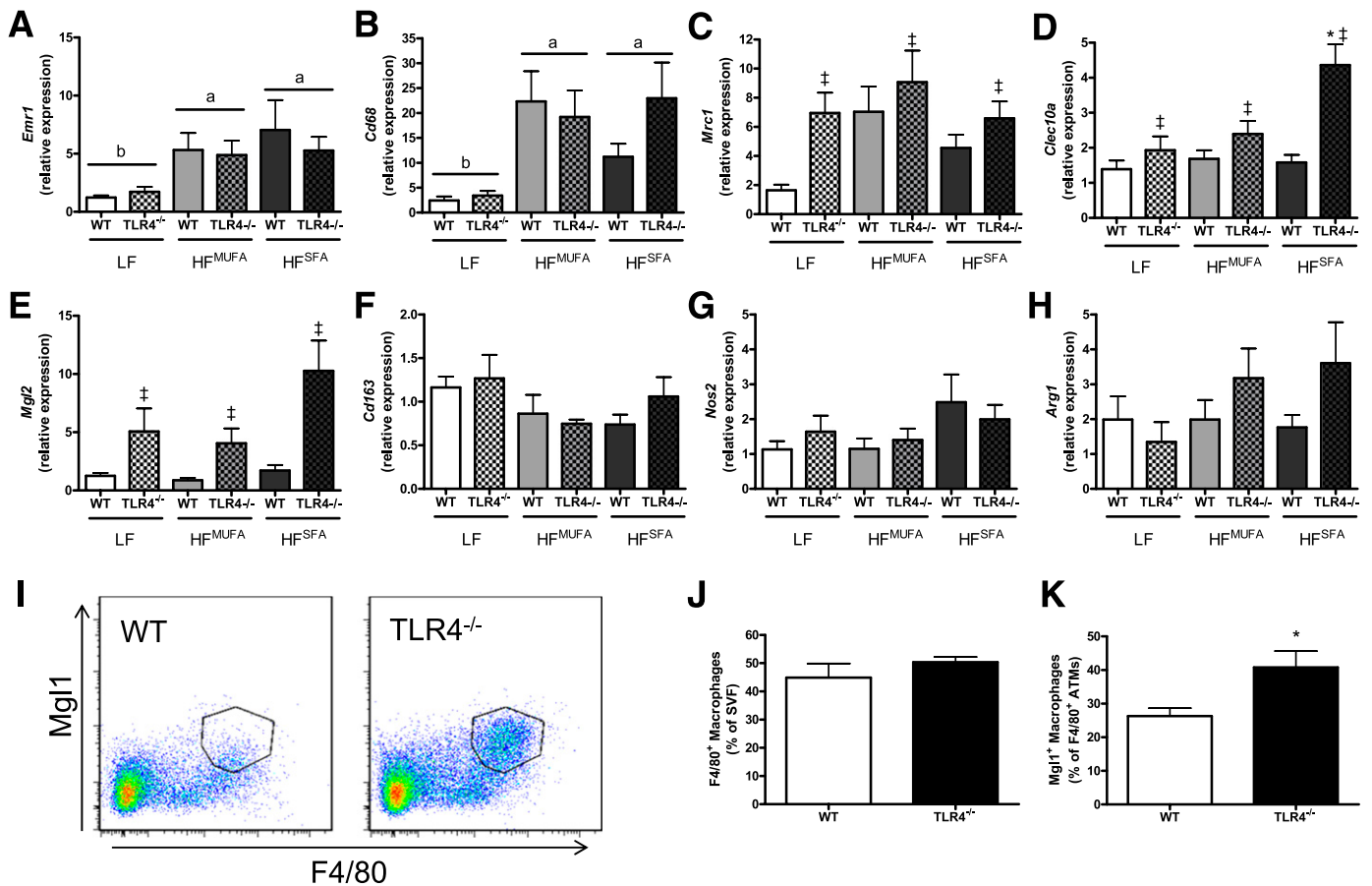
FIG. 3. TLR4 deficiency promotes alternative activation of ATMs. Real-time RT-PCR was used to assess AT mRNA expression of *Emr1* (*A*), *Cd68* (*B*), *Mrc1* (*C*), *Clec10a* (*D*), *Mgl2* (*E*), *Cd163* (*F*), *Nos2* (*G*), and *Arg1* (*H*) ($n = 7$–16). *I*: Representative FACS plot of F4/80$^+$Mgl1$^+$ ATMs from HF^{SFA}-fed WT and TLR4$^{-/-}$ mice. *J*: Quantification of F4/80$^+$ ATMs from HF^{SFA}-fed WT and TLR4$^{-/-}$ mice ($n = 6$–9). *K*: Quantification of F4/80$^+$Mgl1$^+$ ATMs from HF^{SFA}-fed WT and TLR4$^{-/-}$ mice ($n = 4$–5). Data are presented as mean ± SEM. *$P < 0.05$ for HF^{SFA} TLR4$^{-/-}$ compared with HF^{SFA} WT; ‡$P < 0.05$ for genotype effect; and $P < 0.05$ for groups not connected by the same letter. (A high-quality color representation of this figure is available in the online issue.)

expression was significantly reduced compared with WT^{WTBM} (Fig. 5*A* and *B*). Likewise, hematopoietic cell TLR4 deficiency reduced SVF *Ccl3* expression in WT recipients (Fig. 5*F*). Thus, reconstitution of WT recipients with TLR4$^{-/-}$ BM reduced AT inflammation. In contrast to WT recipients, hematopoietic cell TLR4 expression did not influence inflammatory gene expression in the AT of TLR4$^{-/-}$ recipients (Fig. 5*A*–*H*), despite exhibiting differential SVF expression of *Tlr2* (Fig. 5*I*).

Hematopoietic cell TLR4 deficiency promotes ATM alternative activation. AT SVF expression of *Emr1* and *Cd68* were used as surrogate markers of ATM accumulation. Whereas *Emr1* expression was not influenced by recipient or hematopoietic cell TLR4 expression, *Cd68* was significantly upregulated in the WT$^{TLR4-/-BM}$ group compared with the WT^{WTBM} group (Fig. 6*B*). Similar to our findings of ATM alternative activation in globally deficient TLR4$^{-/-}$ mice, hematopoietic cell TLR4 deficiency resulted in significantly greater *Clec10a*, *Mgl2*, and *Mrc1* expression in WT recipients (Fig. 6*C*–*E*). Likewise, TLR4$^{-/-TLR4-/-BM}$ mice displayed elevated expression of *Clec10a* and *Mrc1* as well as reduced expression of *Nos2* compared with TLR4$^{-/-WTBM}$ (Fig. 6*C, E,* and *F*). SVF expression of *Il10* was significantly reduced in WT$^{TLR4-/-BM}$ mice compared with WT^{WTBM} mice (Fig. 6*H*).

Hematopoietic cell TLR4 deficiency does not influence systemic insulin sensitivity. To determine the contribution of parenchymal and hematopoietic cell TLR4 expression to the metabolic response to a HF^{SFA} diet challenge, as well as to account for any significant baseline differences, mice from each BMT group underwent a glucose tolerance test (GTT) before the BMT procedure, and a GTT and insulin tolerance test (ITT) after 20 weeks of HF^{SFA} feeding. Before BMT, all groups exhibited similar glucose excursion curves during the GTT (Fig. 7*A*). In contrast, TLR4$^{-/-}$ recipient groups displayed impaired glucose tolerance compared with WT recipients, regardless of hematopoietic cell TLR4 expression (Fig. 7*B*). In addition, IR, as assessed by ITT, was significantly greater in the TLR4$^{-/-}$ recipient groups than in WT groups; again, hematopoietic TLR4 deficiency had no effect on insulin sensitivity (Fig. 7*C*). A significant recipient × BM genotype interaction was observed for fasting blood glucose as shown by significantly greater concentrations in WT$^{TLR4-/-BM}$ than in WT^{WTBM} (Fig. 7*D*). Plasma insulin was significantly elevated in WT recipients and was not influenced by hematopoietic cell TLR4 expression (Fig. 7*E*).

DISCUSSION

The primary findings of the current study are that global TLR4 deficiency reduces AT inflammation concomitant
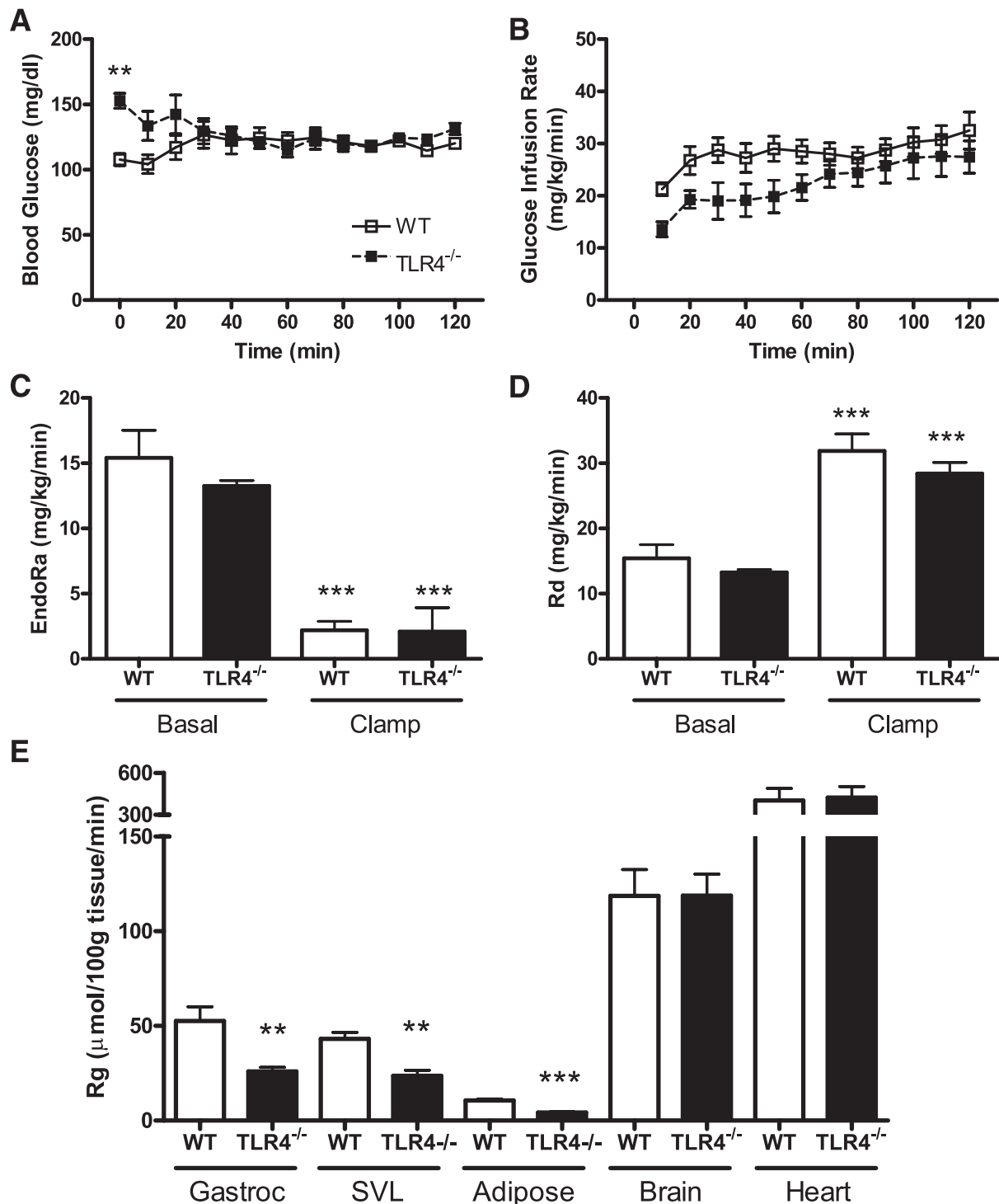
FIG. 4. TLR4 deficiency does not attenuate systemic IR after HF^{SFA} feeding. A: Time course of blood glucose throughout the hyperinsulinemic-euglycemic clamp is presented to illustrate clamp quality. B: The glucose infusion rate required to maintain blood glucose between 120 and 130 mg/dL did not differ between HF^{SFA}-fed TLR4$^{-/-}$ and WT mice. WT and TLR4$^{-/-}$ mice displayed similar rates of endogenous glucose production (EndoR$_a$) (C) and glucose disappearance (R$_d$) (D). E: Glucose uptake (R$_g$) was significantly reduced in the gastrocnemius (Gastroc), superficial vastus lateralis (SVL), and AT of TLR4$^{-/-}$ mice compared with WT. Data are presented as mean ± SEM (n = 4–7). **P < 0.01 and ***P < 0.0001 for TLR4$^{-/-}$ compared with WT.

with a shift in ATM polarization toward an alternatively activated state. To our knowledge, this is the first direct experimental evidence for a role of TLR4 in ATM polarization, which is further supported by the finding that hematopoietic cell TLR4 deficiency is sufficient to elicit the alternative activation of ATMs irrespective of recipient genotype.

Despite using a dietary strategy aimed at maximizing our ability to detect TLR4-dependent effects of dietary SFA content, we failed to observe a robust difference in the metabolic or inflammatory response of TLR4$^{-/-}$ mice to the HF^{MUFA} and HF^{SFA} diets. Results of previous studies suggesting that SFAs directly activate TLR4 (4,24,25) have been questioned. A
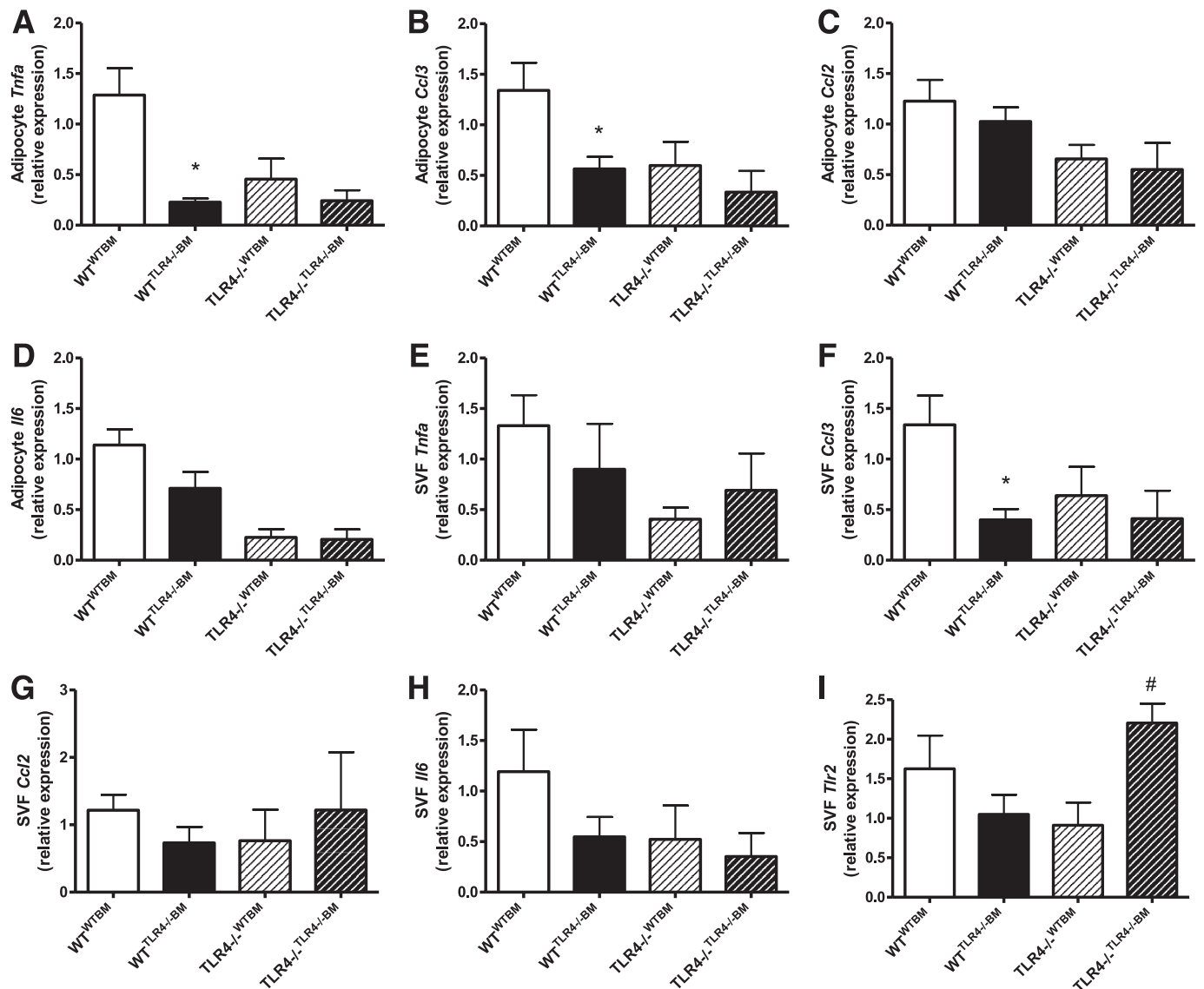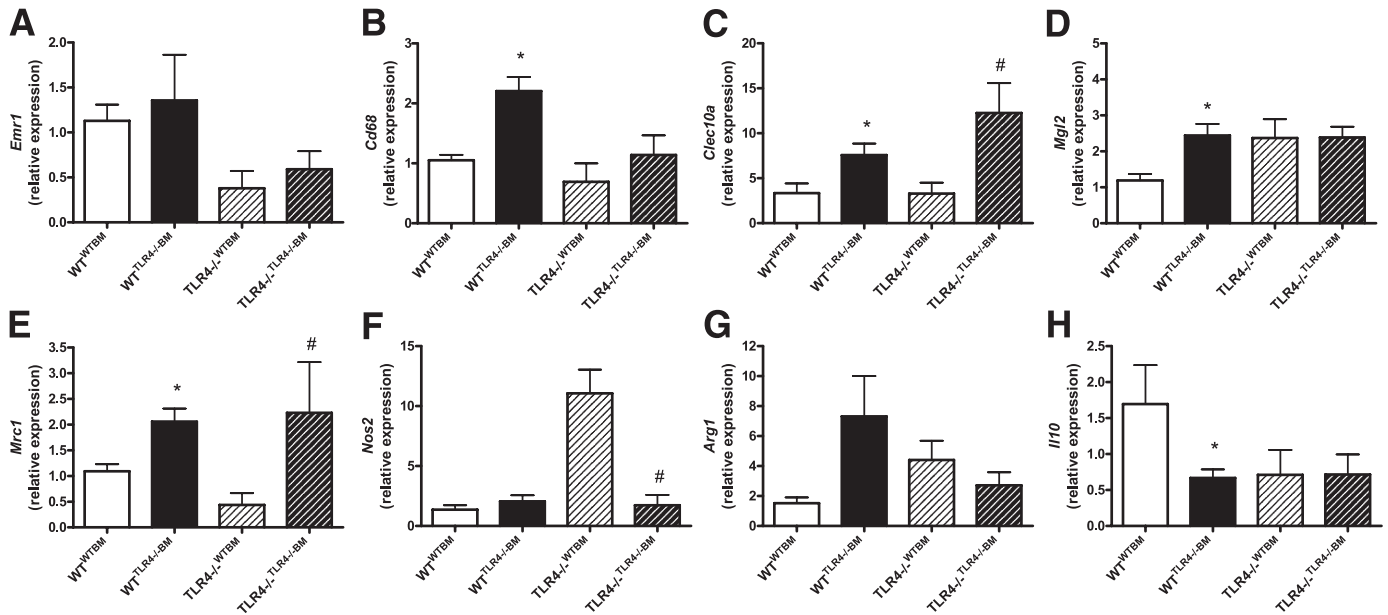
FIG. 5. Hematopoietic cell TLR4 deficiency attenuates AT inflammation in WT recipient mice. Real time RT-PCR was used to assess adipocyte fraction mRNA expression of *Tnfa* (*A*), *Ccl3* (*B*), *Ccl2* (*C*), and *Il6* (*D*) as well as SVF mRNA expression of *Tnfa* (*E*), *Ccl3* (*F*), *Ccl2* (*G*), *Il6* (*H*), and *Tlr2* (*I*). Data are presented as mean ± SEM (n = 7–16). *$P < 0.05$ for WT$^{TLR4-/-BM}$ compared with WT^{WTBM}, and #$P < 0.01$ for TLR4$^{-/-TLR4-/-BM}$ compared with TLR4$^{-/-WTBM}$.

recent report by Erridge and Samani (27) demonstrates that lipopolysaccharide and lipopeptide contamination of BSA accounts for the TLR4 activation commonly attributed to SFA treatment. We recognize that the current study does not directly address this issue; however, our findings do not generally support the notion that dietary SFAs directly induce TLR4 signaling. Irrespective of whether SFAs act as a TLR4 ligand, several lines of evidence suggest a much more complex and multifaceted immunomodulatory role for dietary fatty acids, such as inducing a shift to gram-negative intestinal microbiota and increasing gut permeability (28).

The finding of reduced weight gain in TLR4$^{-/-}$ mice after HF feeding is in line with some (5,7,26,29)—but not all—previous investigations (6,10–12,30,31). Careful examination of the available literature highlights the difficulty in drawing direct comparisons between previous studies because important differences exist with respect to *1*) sex and age of the mice used; *2*) percentage of dietary fat (ranging from 42–60% kcal from fat); *3*)

carbohydrate source (e.g., sucrose or corn starch); *4*) TLR4-deficient model (i.e., C57BL/10ScN, C3H/HeJ, or TLR4$^{-/-}$ mice on a BL/6 or BL/10 background); and *5*) study duration. Unfortunately, no discernible patterns exist that might explain the various weight gain results. Taken in context with the current literature, our study suggests that any protection TLR4 deficiency may confer with respect to weight gain is likely very modest and of questionable physiologic relevance.

Our results are in agreement with the general consensus of previous studies demonstrating a reduction in hepatic lipid accumulation in TLR4$^{-/-}$ mice after HF feeding (5–7). Perhaps surprising was the lack of effect noted in our BMT model with respect to the influence of parenchymal or hematopoietic cell TLR4 deficiency on hepatic steatosis. Whereas we observed similar levels of hepatic TG accumulation in WT and TLR4$^{-/-}$ recipients, regardless of hematopoietic cell TLR4 expression, Saberi et al. (32) recently reported a dramatic reduction in hepatic TG concentrations after

FIG. 6. Hematopoietic cell TLR4 deficiency promotes the alternative activation of ATMs. Real-time RT-PCR was used to assess SVF mRNA expression of *Emr1* (*A*), *Cd68* (*B*), *Clec10a* (*C*), *Mgl2* (*D*), *Mrc1* (*E*), *Nos2* (*F*), *Arg1* (*G*), and *Il10* (*H*). Data are presented as mean ± SEM (n = 7–16). *$P < 0.05$ for WT$^{TLR4-/-BM}$ compared with WT^{WTBM}, and #$P < 0.05$ for TLR4$^{-/-TLR4-/-BM}$ compared with TLR4$^{-/-WTBM}$.

HF feeding in WT mice reconstituted with TLR4$^{-/-}$ BM. The reasons for this inconsistency are unclear but likely include differences in diet and the duration of HF feeding.

Similar to previous investigations (10–13), we found that global as well as hematopoietic cell TLR4 deficiency produces modest reductions in AT inflammation despite comparable increases in ATM accumulation after HF feeding, suggesting that the absence of TLR4 signaling may influence ATM phenotype. Support for this possibility comes from the finding that the expression of various
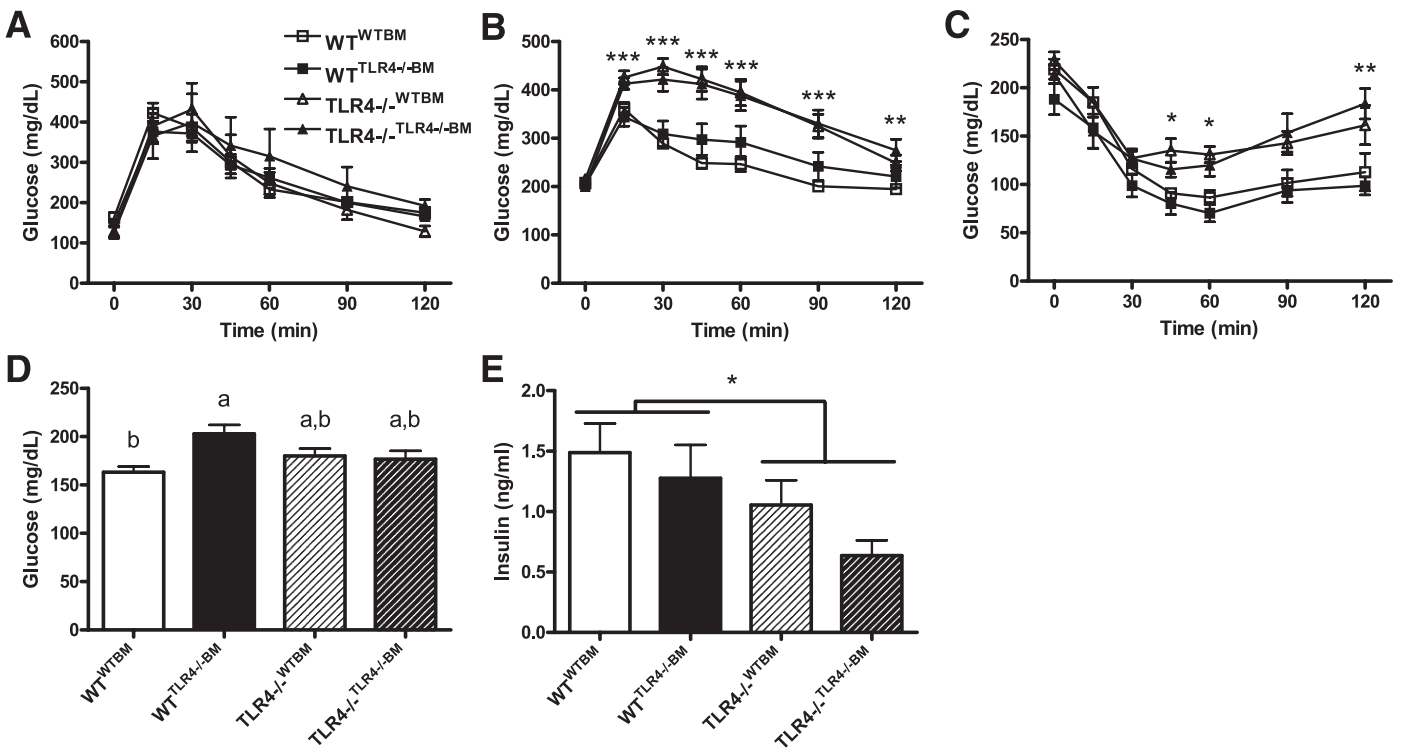
FIG. 7. *A*: Hematopoietic cell TLR4 deficiency does not influence systemic insulin sensitivity. WT and TLR4$^{-/-}$ mice displayed similar glucose excursion curves before BMT (n = 5–9). After 20 weeks of an HF^{SFA} diet, TLR4$^{-/-}$ recipient mice exhibited impaired glucose (n = 8–15) (*B*) and insulin (n = 6–8) (*C*) tolerance compared with WT recipients, regardless of hematopoietic cell TLR4 expression. *D*: Fasting blood glucose (n = 8–18). *E*: Fasting plasma insulin (n = 8–18). Data are presented as mean ± SEM. *$P < 0.05$, **$P < 0.01$, and ***$P < 0.001$ for recipient genotype effect, and $P < 0.05$ for groups not connected by the same letter.

markers of M2 macrophage polarization are elevated in the AT of TLR4$^{-/-}$ mice. Likewise, the proportion of M2 ATMs (i.e., F4/80$^+$Mgl1$^+$) is significantly greater in HF^{SFA}-fed TLR4$^{-/-}$ mice than in WT counterparts. Interestingly, our BMT model points to a direct influence of TLR4 signaling on ATM polarization, as shown by the elevation of M2 marker expression in the SVF of mice reconstituted with TLR4$^{-/-}$ BM, regardless of recipient genotype (i.e., WT$^{TLR4-/-BM}$ and TLR4$^{-/-TLR4-/-BM}$). Additional support for a direct role of TLR4 in macrophage polarization comes from the finding that TLR4$^{-/-}$ PMs are skewed toward an alternatively activated expression profile. In addition to the potential for TLR4 deficiency to directly modulate ATM polarization, the possibility that the alternative activation observed in TLR4-deficient ATMs may actually represent a relative resistance to the shift in ATM polarization toward an M1 phenotype in response to elevated endotoxin concentrations during HF feeding should not be discounted.

Despite displaying reductions in body weight, hepatic steatosis, and AT inflammation, we failed to detect any beneficial impact of TLR4 deficiency on systemic IR. Although previous studies have reported a lack of TLR4 signaling (via knockout or loss-of-function mutation) attenuates lipid infusion–induced IR (5,10,33), the effect of TLR4 deficiency on insulin sensitivity in the setting of DIO remains unclear. Regarding these inconsistencies, it is interesting to note that those studies reporting an attenuation of IR after an HFD used diets providing 55–60% kcal from fat (7,10,11), whereas studies (including the present) using diets consisting of 42–45% kcal from fat consistently fail to show an effect of TLR4 deficiency on IR (5,6). This raises the possibility that our ability to detect the influence of TLR4 on systemic insulin sensitivity was compromised by the use of 45% fat diets.

Similar to models of global TLR4 deficiency, the role of hematopoietic cell TLR4 signaling in HFD-induced IR is uncertain. Olefsky and colleagues (32) recently reported that hematopoietic cell TLR4 deficiency, as well as lentiviral mediated knockdown of TLR4 in hematopoietic cells, attenuates IR after HF feeding. In contrast, the current study and a previous report by our laboratory (13) both failed to detect an improvement in systemic insulin sensitivity in mice lacking hematopoietic TLR4 signaling. Notably, TLR4$^{-/-}$ recipients (i.e., TLR4$^{-/-WTBM}$ and TLR4$^{-/-TLR4-/-BM}$) were significantly more glucose- and insulin-intolerant than WT recipients (i.e., WT^{WTBM} and WT$^{TLR4-/-BM}$), regardless of hematopoietic cell TLR4 expression. Because previous studies have only used WT recipients, we are unable to reconcile this unexpected finding. Nonetheless, this does not impact our finding that hematopoietic cell TLR4 deficiency does not influence glucose or insulin tolerance.

In summary, the current study demonstrates that TLR4 deficiency promotes the alternative activation of ATMs. Furthermore, the alternative activation of ATMs in hematopoietic cell TLR4–deficient chimeras suggests that TLR4 signaling plays a direct role in mediating ATM phenotype in DIO. Lastly, it should be emphasized that, despite the observed influence on ATM phenotype and AT inflammation, in our hands, global and hematopoietic TLR4 deficiency produces a modest phenotype that does not manifest in improved systemic glucose homeostasis.

REFERENCES

1. Hotamisligil GS, Shargill NS, Spiegelman BM. Adipose expression of tumor necrosis factor-alpha: direct role in obesity-linked insulin resistance. Science 1993;259:87–91
2. Gregor MF, Hotamisligil GS. Inflammatory mechanisms in obesity. Annu Rev Immunol 2011;29:415–445
3. Medzhitov R, Preston-Hurlburt P, Janeway CA Jr. A human homologue of the *Drosophila* Toll protein signals activation of adaptive immunity. Nature 1997;388:394–397
4. Lee JY, Sohn KH, Rhee SH, Hwang D. Saturated fatty acids, but not unsaturated fatty acids, induce the expression of cyclooxygenase-2 mediated through Toll-like receptor 4. J Biol Chem 2001;276:16683–16689
5. Radin MS, Sinha S, Bhatt BA, Dedousis N, O'Doherty RM. Inhibition or deletion of the lipopolysaccharide receptor Toll-like receptor-4 confers partial protection against lipid-induced insulin resistance in rodent skeletal muscle. Diabetologia 2008;51:336–346
6. Poggi M, Bastelica D, Gual P, et al. C3H/HeJ mice carrying a toll-like receptor 4 mutation are protected against the development of insulin resistance in white adipose tissue in response to a high-fat diet. Diabetologia 2007;50:1267–1276
7. Tsukumo DML, Carvalho-Filho MA, Carvalheira JBC, et al. Loss-of-function mutation in Toll-like receptor 4 prevents diet-induced obesity and insulin resistance. Diabetes 2007;56:1986–1998
8. Olefsky JM, Glass CK. Macrophages, inflammation, and insulin resistance. Annu Rev Physiol 2010;72:219–246
9. Suganami T, Ogawa Y. Adipose tissue macrophages: their role in adipose tissue remodeling. J Leukoc Biol 2010;88:33–39
10. Shi H, Kokoeva MV, Inouye K, Tzameli I, Yin H, Flier JS. TLR4 links innate immunity and fatty acid-induced insulin resistance. J Clin Invest 2006;116:3015–3025
11. Suganami T, Mieda T, Itoh M, Shimoda Y, Kamei Y, Ogawa Y. Attenuation of obesity-induced adipose tissue inflammation in C3H/HeJ mice carrying a Toll-like receptor 4 mutation. Biochem Biophys Res Commun 2007;354:45–49
12. Suganami T, Yuan X, Shimoda Y, et al. Activating transcription factor 3 constitutes a negative feedback mechanism that attenuates saturated fatty acid/Toll-like receptor 4 signaling and macrophage activation in obese adipose tissue. Circ Res 2009;105:25–32
13. Coenen KR, Gruen ML, Lee-Young RS, Puglisi MJ, Wasserman DH, Hasty AH. Impact of macrophage Toll-like receptor 4 deficiency on macrophage infiltration into adipose tissue and the artery wall in mice. Diabetologia 2009;52:318–328
14. Morris DL, Singer K, Lumeng CN. Adipose tissue macrophages: phenotypic plasticity and diversity in lean and obese states. Curr Opin Clin Nutr Metab Care 2011;14:341–346
15. Westcott DJ, Delproposto JB, Geletka LM, et al. MGL1 promotes adipose tissue inflammation and insulin resistance by regulating 7/4hi monocytes in obesity. J Exp Med 2009;206:3143–3156

16. Coenen KR, Gruen ML, Chait A, Hasty AH. Diet-induced increases in adiposity, but not plasma lipids, promote macrophage infiltration into white adipose tissue. Diabetes 2007;56:564–573
17. Saraswathi V, Hasty AH. Inhibition of long-chain acyl coenzyme A synthetases during fatty acid loading induces lipotoxicity in macrophages. Arterioscler Thromb Vasc Biol 2009;29:1937–1943
18. Surmi BK, Webb CD, Ristau AC, Hasty AH. Absence of macrophage inflammatory protein-1α does not impact macrophage accumulation in adipose tissue of diet-induced obese mice. Am J Physiol Endocrinol Metab 2010;299:E437–E445.
19. Saraswathi V, Hasty AH. The role of lipolysis in mediating the proinflammatory effects of very low density lipoproteins in mouse peritoneal macrophages. J Lipid Res 2006;47:1406–1415
20. Saraswathi V, Morrow JD, Hasty AH. Dietary fish oil exerts hypolipidemic effects in lean and insulin sensitizing effects in obese LDLR-/- mice. J Nutr 2009;139:2380–2386
21. Ayala JE, Bracy DP, McGuinness OP, Wasserman DH. Considerations in the design of hyperinsulinemic-euglycemic clamps in the conscious mouse. Diabetes 2006;55:390–397
22. Ayala JE, Bracy DP, Julien BM, Rottman JN, Fueger PT, Wasserman DH. Chronic treatment with sildenafil improves energy balance and insulin action in high fat-fed conscious mice. Diabetes 2007;56:1025–1033
23. Fueger PT, Bracy DP, Malabanan CM, Pencek RR, Wasserman DH. Distributed control of glucose uptake by working muscles of conscious mice: roles of transport and phosphorylation. Am J Physiol Endocrinol Metab 2004;286:E77–E84
24. Lee JY, Ye J, Gao Z, et al. Reciprocal modulation of Toll-like receptor-4 signaling pathways involving MyD88 and phosphatidylinositol 3-kinase/AKT by saturated and polyunsaturated fatty acids. J Biol Chem 2003;278:37041–37051
25. Hwang D. Modulation of the expression of cyclooxygenase-2 by fatty acids mediated through toll-like receptor 4-derived signaling pathways. FASEB J 2001;15:2556–2564
26. Milanski M, Degasperi G, Coope A, et al. Saturated fatty acids produce an inflammatory response predominantly through the activation of TLR4 signaling in hypothalamus: implications for the pathogenesis of obesity. J Neurosci 2009;29:359–370
27. Erridge C, Samani NJ. Saturated fatty acids do not directly stimulate Toll-like receptor signaling. Arterioscler Thromb Vasc Biol 2009;29:1944–1949
28. Cani PD, Bibiloni R, Knauf C, et al. Changes in gut microbiota control metabolic endotoxemia-induced inflammation in high-fat diet-induced obesity and diabetes in mice. Diabetes 2008;57:1470–1481
29. Davis JE, Gabler NK, Walker-Daniels J, Spurlock ME. Tlr-4 deficiency selectively protects against obesity induced by diets high in saturated fat. Obesity (Silver Spring) 2008;16:1248–1255
30. Vijay-Kumar M, Aitken JD, Carvalho FA, Ziegler TR, Gewirtz AT, Ganji V. Loss of function mutation in Toll-like receptor-4 does not offer protection against obesity and insulin resistance induced by a diet high in trans fat in mice. J Inflamm (Lond) 2011;8:2
31. Kim F, Pham M, Luttrell I, et al. Toll-like receptor-4 mediates vascular inflammation and insulin resistance in diet-induced obesity. Circ Res 2007;100:1589–1596
32. Saberi M, Woods N-B, de Luca C, et al. Hematopoietic cell-specific deletion of Toll-like receptor 4 ameliorates hepatic and adipose tissue insulin resistance in high-fat-fed mice. Cell Metab 2009;10:419–429
33. Holland WL, Bikman BT, Wang LP, et al. Lipid-induced insulin resistance mediated by the proinflammatory receptor TLR4 requires saturated fatty acid-induced ceramide biosynthesis in mice. J Clin Invest 2011;121:1858–1870